Title

Hypoxia-induced pulmonary hypertension in type 2 diabetic mice

Journal

Pulmonary Circulation, 7(1)

ISSN

2045-8932

Authors

Pan, Minglin
Han, Ying
Si, Rui
et al.

Publication Date

2017

DOI

10.1086/690206

Peer reviewed

Research Article

Pulmonary Circulation

Hypoxia-induced pulmonary hypertension in type 2 diabetic mice

Minglin Pan[1,2], Ying Han[1,3], Rui Si[3], Rui Guo[3], Ankit Desai[1,3] and Ayako Makino[1,3]

[1]Department of Medicine, University of Illinois at Chicago, Chicago, IL, USA; [2]Department of Endocrinology, The Second Affiliated Hospital of Nanjing Medical University, Nanjing, China; [3]Department of Physiology, University of Arizona, Tucson, AZ, USA

Abstract

Hypoxia-induced pulmonary hypertension (HPH) is a progressive disease that is mainly caused by chronic exposure to high altitude, chronic obstructive lung disease, and obstructive sleep apnea. The increased pulmonary vascular resistance and increased pulmonary arterial pressure result in increased right ventricular afterload, leading to right heart failure and increased morbidity. There are several clinical reports suggesting a link between PH and diabetes, insulin resistance, or obesity; however, it is unclear whether HPH is associated with diabetes as a progressive complication in diabetes. The major goal of this study is to examine the effect of diabetic "preconditioning" or priming effect on the progression of HPH and define the molecular mechanisms that explain the link between diabetes and HPH. Our data show that HPH is significantly enhanced in diabetic mice, while endothelium-dependent relaxation in pulmonary arteries is significantly attenuated in chronically hypoxic diabetic mice (DH). In addition, we demonstrate that mouse pulmonary endothelial cells (MPECs) isolated from DH mice exhibit a significant increase in mitochondrial reactive oxygen species (ROS) concentration and decreased SOD2 protein expression. Finally, scavenging mitochondrial ROS by mitoTempol restores endothelium-dependent relaxation in pulmonary arteries that is attenuated in DH mice. These data suggest that excessive mitochondrial ROS production in diabetic MPECs leads to the development of severe HPH in diabetic mice exposed to hypoxia.

Keywords

pulmonary artery, endothelial cell, mitochondria, reactive oxygen species (ROS), endothelium-dependent relaxation

Date received: 13 October 2016; accepted: 16 November 2016

Pulmonary Circulation 2017; 7(1) 175–185
DOI: 10.1086/690206

In the USA, more than 29 million people suffer from diabetes and 1.7 million people, aged 20 years or older, are newly diagnosed with diabetes every year. Diabetes is the seventh leading cause of death and nearly 65% of patients with diabetes die from cardiovascular diseases. Because of such a large diabetic population, many diabetic patients living in areas of high altitudes or having hypoxic lung diseases (e.g. chronic obstructive pulmonary disease [COPD]) and obstructive sleep apnea (OSA) might be exposed to sustained hypobaric hypoxia (in high altitudes), regional alveolar hypoxia (due to COPD), and intermittent hypoxia (as a result of OSA).

Hypoxia is a major cause for pulmonary hypertension (PH). Hypoxia-induced pulmonary hypertension (HPH) or PH associated with hypoxic lung diseases is categorized as World Health Organization (WHO) Group III of PH and is mainly associated with chronic exposure to high altitudes, chronic obstructive lung disease (e.g. COPD), and OSA. The first clinical report that documented the link between diabetic mellitus (DM) and PH was published in 2005.[1] Mavahed et al. showed that patients with DM exhibited a significantly higher prevalence of PH than in non-diabetic patients. Later, Makarevich et al. demonstrated that mean pulmonary arterial pressure (PAP) was significantly higher in patients with DM and COPD than in patients with COPD alone.[2] Pugh et al. reported that PH patients with higher HbA1c (>6.0%) showed shorter 6-minute walk

Corresponding author:
Ayako Makino, Department of Physiology, University of Arizona, 1501 N. Campbell Ave., PO Box 245051, Tucson, AZ 85724, USA.
Email: aymakino@email.arizona.edu

distance (a method to assess the disease condition and therapeutic outcome in PH patients) compared to PH patients with <6.0% HbA1c.[3] The survival rate in PH patients with DM was also worse than in PH patients without DM.[4,5] These data clearly indicate that there is a strong correlation between DM and the progression or severity of PH. The molecular mechanisms to increase the susceptibility to the hypoxia in diabetes are, however, not revealed.

Vascular endothelial cells play an important role in the regulation of vascular tone and formation of new vessels. Vasoconstriction and vasodilatation are regulated by the endothelium via secretion of endothelium-derived constricting factors (e.g. thromboxane A_2 and endothelin-1) and endothelium-derived relaxing factors (e.g. nitric oxide [NO], prostacyclin [PGI_2], and endothelium-derived hyperpolarizing factors [EDHF]). Endothelium-dependent hyperpolarization (EDH) is also an important mechanism that leads to endothelium-dependent vasodilation. It is well demonstrated that the endothelium is dysfunctional in diabetes[6–9] and the endothelium-dependent relaxation (EDR) is attenuated due to the decrease in NO bioavailability[10–13] and/or impaired EDH-induced relaxation.[14–16] Pulmonary endothelial dysfunction is also implicated in the development and progression of PH.[17–19] Therefore, pulmonary vascular endothelial dysfunction associated with diabetes would inhibit pulmonary EDR, which subsequently results in sustained vasoconstriction and ultimately increases pulmonary vascular resistance (PVR) and PAP.

Under physiological conditions, ECs constantly generate reactive oxygen species (ROS), including superoxide anion ($O_2^{-\bullet}$), that participate in modulation of essential endothelial functions. The imbalance between production and elimination of ROS results in increased oxidative stress and tissue injury, and leads to many cardiovascular diseases. The putative sources of $O_2^{-\bullet}$ include mitochondrial respiratory chain,[20] uncoupled eNOS,[21] NADPH oxidases,[22] and xanthine oxidase. It has been reported that altered mitochondrial $O_2^{-\bullet}$ concentration ($[O_2^{-\bullet}]_{mito}$) is involved in endothelial dysfunction in diabetes[12,23–28] and PH;[29–33] however, there is no report investigating the mitochondrial ROS concentration ($[ROS]_{mito}$) under both hypoxia and diabetic conditions. In this study, we demonstrate that diabetic mice are more susceptive to hypoxia to develop severe PH compared to non-diabetic mice. It is, at least in part, caused by increased $[ROS]_{mito}$ in pulmonary endothelial cells and decreased endothelium-dependent pulmonary vasodilation in diabetic mice under hypoxia. Our data imply that diabetic patients who live in the high altitude, suffer from hypoxic respiratory diseases like COPD or have OSA might have a higher risk of developing severe PH.

Methods

Biological materials and reagents

M199, antibiotic reagents, dispase II, and MitoSOX Red were purchased from Thermo Fisher Scientific Inc. (Rockford, IL, USA). Streptozotocin and anti-superoxide dismutase 2 (SOD2) antibody were obtained from Enzo Life Science (Plymouth Meeting, PA, USA). Anti-actin antibody and mitoTempol (mitoT) were obtained from Santa Cruz Biotechnology (Santa Cruz, CA, USA). Anti-CD31 and endothelial cell growth supplement (ECGS) were purchased from BD Biosciences (San Jose, CA, USA). Collagenase II was from Worthington Biochemical (Lakewood, NJ, USA), and Microfil compound (yellow) was purchased from Flowtech Inc. (South Windsor, CT, USA). All other chemicals were obtained from Sigma-Aldrich (St Louis, MO, USA).

Animal experiment

This animal study was conducted in accordance with the guidelines established by the Institutional Animal Care and Use Committee (IACUC) at the University of Arizona. All animal use is in compliance with all current US government regulations concerning the care and use of laboratory animals. The University of Arizona has been certified (Animal Welfare Assurance #A3248-01) and the approved protocol number for this study is #14-520. The laboratory personnel who conducted the following animal experiments took all training courses required for animal handling and were certified by the IACUC. All surgery was performed under anesthesia with a mixture of ketamine (100 mg/kg, i.p.) and xylazine (5 mg/kg, i.p.), and all efforts were made to minimize suffering.

Male C57BL/6 mice were purchased from the Jackson Laboratory (Bar Harbor, ME, USA). Inducible type 2 diabetic (T2D) mice were generated by a single injection of streptozotocin (STZ, 75 mg/kg, dissolved in citrate buffer, i.p.) at the age of 6 weeks, and given a high fat diet (HF, 60% kcal) from the day of the STZ injection.[34,35] Genetically modified T2D mice (KK.Cg-A^y/a mice: KK mice) were purchased from the Jackson Laboratory and bred in-house. For HPH mouse experiments, mice were exposed to hypoxia (10% O_2) in a ventilated chamber for four weeks to develop PH.

Oral glucose tolerance test (OGTT)

OGTT was performed as described previously.[34,36] Briefly, mice were fasted for 6 h before the OGTT. Glucose (2 g/kg bwt) was administrated orally and plasma glucose concentration was measured at time 0 (before glucose administration), 15, 30, and 60 min after glucose administration.

Right ventricle systolic pressure (RVSP) measurement

After mice were anesthetized, a catheter was inserted into the right external jugular vein. Right ventricular pressure (RVP) was measured and recorded using a MPVS Ultra system (Millar Instruments) as described in our previous manuscript.[37] RVSP was calculated and compared between

control and diabetic mice. We also calculated the change of RVSP (normalized data by normoxia control [DN-CN, CH-CN, DH-CN]).

Lung angiograph

Pulmonary angiography was conducted to visualize the pulmonary vascular tree in the mouse lung using Microfil. The lungs were perfused with 0.5 mL/min Microfil for 2 min through the pulmonary artery (PA) and fixed at 4°C for overnight. Then the lungs filled with Microfil were bathed in serial concentrations of ethanol, placed in methyl salicylate, and photographed with a digital camera (MD600E, Amscope, Irvine, CA, USA). We made binary images using NIH ImageJ 1.48v software on the peripheral pulmonary vasculature (the areas between the edge of the lung and 1 mm inside from the edge of the lung) using Photoshop CS software; the images were then skeletonized for analyzing the number of vessel branches, the number of junctions, and the total length. These data were normalized by the area selected in each lung image.

Isometric tension measurement in isolated PA ring

Isometric tension was measured as previously described.[36] The lung was isolated and placed in Krebs-Henseleit solution for dissection. The third-order small PAs were dissected out of the lung; attached fat and adherent connective tissues were then removed from the isolated PA rings. The PA rings were cut into 1–1.5-mm long segments. Rings were mounted on a wire myograph with stainless wires of 20 μm in diameter; the resting tension of the isolated PA ring was set at 100 mg (DMT-USA, Inc.). All PA rings set at the resting tension were equilibrated for 45 min with intermittent washes every 15 min. After equilibration, each PA ring was precontracted by application of $PGF_2\alpha$, and the degree of ACh-induced vasodilatation was described as a percentage (%) decrease of $PGF_2\alpha$-induced contraction.

Isolation of mouse pulmonary endothelial cells (MPEC)

MPECs were isolated as previously described.[36] Briefly, dissected lung tissues were minced and incubated in M199 containing 2 mg/mL collagenase I and 0.6 U/mL dispase II for 1 h at 37°C. The digested material, including single cells and pieces of tissue, was filtered through sterile 70-μm nylon mesh and washed in M199 containing 2% fetal calf serum. The remaining cells were then incubated with Dynabeads (Invitrogen) coated with CD31 antibody. The Dynabeads were prepared as follows: beads coated with sheep anti-rat antibody were incubated with purified rat anti-mouse CD31 monoclonal antibody (1 μg/mL) at 4°C overnight and then washed with PBS containing 0.1% BSA and 2 mM EDTA. Cell suspension was incubated with the CD31 antibody-coated beads for 1 h at 4°C and then beads attached to endothelial cells were captured by Dynal magnet (Invitrogen).

Measurement of mitochondrial ROS concentration

$[ROS]_{mito}$ was measured as described previously.[24,38] Mitochondrial ROS was detected by preloading the cells with 5 μmol/L of MitoSOX Red (mitochondrial ROS indicator) for 30 min. MitoSOX fluorescence from the cells were imaged using a Nikon Eclipse Ti-E inverted fluorescence microscope with 60 × objective lens. The fluorescence intensity of the MitoSOX in the mitochondria was measured and the background intensity was subtracted from the cell intensity.

Western blot analysis

Isolated MPECs were lysed and centrifuged at 16,000 g for 10 min at 4°C. Protein samples from ECs were separated through a SDS-polyacrylamide gel and transferred to the membranes. Blots were incubated with a primary antibody (anti-SOD2 [1:1000] or anti-actin [1:4000]) followed by incubation with a HRP-conjugated secondary antibody. The immunoblots were detected with Super Signal West Pico reagent (Thermo Fisher Scientific Inc. Rockford, IL, USA). Band intensity was normalized to actin control and expressed in arbitrary units.

Statistical analysis

The data are expressed as means ± standard error (SEM). Differences between groups were analyzed for statistical significance using Student's *t*-test and post-hoc ANOVA. Differences were considered to be statistically significant when a P value was less than 0.05 ($P < 0.05$).

Results

Effect of chronic hypoxia exposure on OGTT and RVSP in inducible T2D mice

To examine whether chronic hypoxia differentially affects control and diabetic mice, we used two different diabetic models: (i) inducible T2D mice (Fig. 1); and (ii) genetically modified T2D (KK mice) (Fig. 2). Fig. 1a shows the time course of the experiments in inducible T2D mice. There were four groups of mice in the experiments: (i) control normoxia (CN) mice; (ii) diabetic normoxia (DN) mice; (iii) control hypoxia (CH) mice; and (iv) diabetic hypoxia (DH) mice. In all groups of mice, we conducted the experimental measurement (e.g. OGTT, RVSP) 16 weeks after initial grouping. In the CN group, the mice were injected with vehicle at the age of 6 weeks and housed in the same room as other mice under normoxic conditions for 16 weeks before the experiment. In the DN group, the mice were injected with STZ and fed with a HF diet at the age of 6 weeks and housed under normoxic conditions for 16 weeks before the experiment. In control hypoxia (CH) group, mice were placed in a normobaric hypoxic chamber at the age of 18 weeks and exposed to hypoxia (10% O_2) for 4 weeks before the experiment.

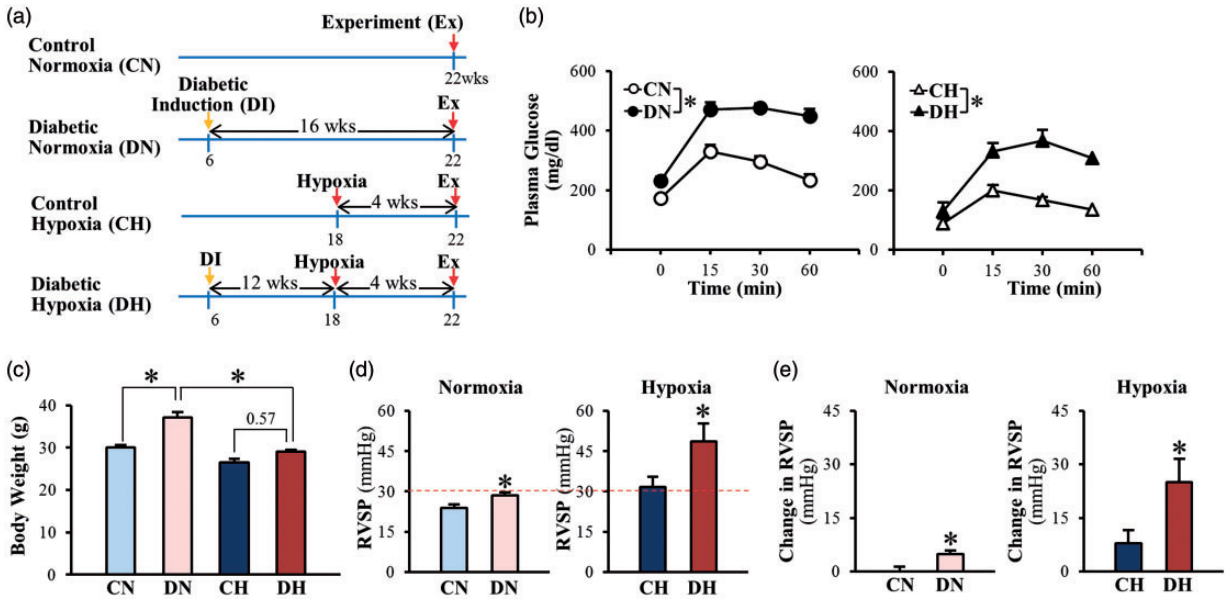

Fig. 1. Inducible T2D mice exhibit higher levels of RVSP than control mice during normoxia and hypoxia-induced increase in RVSP is more prominent in T2D mice compared to control mice. (a) Proposed experimental groups and protocols in mice. CN, control normoxia; DN, diabetic normoxia; CH, control hypoxia; DH, diabetic hypoxia. (b) Oral glucose tolerance test. T2D mice exhibit abnormal glucose tolerance curve under normoxia and hypoxia. CN, n = 10; DN, n = 10; CH, n = 7; DH; n = 7. Data are mean ± SEM. *$P < 0.05$ vs. control mice. (c) Body weight. Hypoxia exposure decreases body weight in T2D mice. CN, n = 10; DN, n = 10; CH, n = 7; DH; n = 7. Data are mean ± SEM. *$P < 0.05$ vs. DN. (d) RVSP. CN, n = 4; DN, n = 4; CH, n = 5; DH; n = 5. Data are mean ± SEM. *$P < 0.05$ vs. control mice. (e). Change in RVSP. CN, n = 4; DN, n = 4; CH, n = 5; DH; n = 5. Data are mean ± SEM. *$P < 0.05$ vs. control mice.

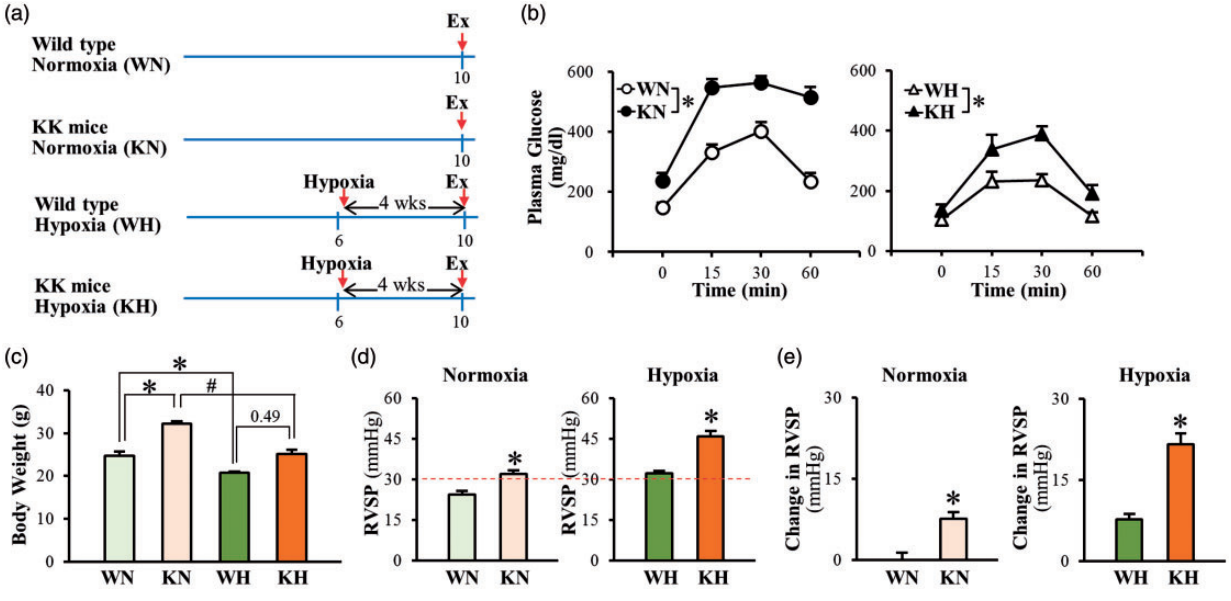

Fig. 2. Chronic hypoxia-exposure increases RVSP in genetically modified type 2 mice (KK mice) greater than in wild-type mice. (a) Proposed experimental groups and protocols in mice. Wild-type normoxia (WN), KK mice normoxia (KN), wild-type hypoxia (WH), and KK mice hypoxia (KH). (b) Oral glucose tolerance test. Hypoxia decreased fasting glucose levels in both wild-type and KK mice; however impaired glucose tolerance still remains in KK mice. WN, n = 5; KN, n = 5; WH, n = 5; KH, n = 4. Data are mean ± SEM. *$P < 0.05$ vs. wild-type mice. (c) Body weight. Mice exposed to hypoxia exhibit lower body weight than mice under normoxia. WN, n = 5; KN, n = 5; WH, n = 5; KH, n = 4. Data are mean ± SEM. *$P < 0.05$ vs. WN, $^{\#}P < 0.05$ vs. KN. (d) RVSP. n = 6 per group. Data are mean ± SEM. *$P < 0.05$ vs. wild-type mice. (e) Change in RVSP. n = 6 per group. Data are mean ± SEM. *$P < 0.05$ vs. wild-type mice.

In the DH group, the mice were injected with STZ and fed with a HF diet at the age of 6 weeks, placed in a normobaric hypoxic chamber at 12 weeks after induction of diabetes, and exposed to hypoxia (10% O_2) for 4 weeks before the experiment.

In control normoxia (CN) mice, glucose tolerance curves showed a normal decline in plasma glucose 30 min after initial glucose intake (at 0 min) (Fig. 1b, open circles), whereas in diabetic normoxia (DN) mice, glucose tolerance was significantly attenuated as shown in the glucose tolerance curve in which the decline phase of the plasma glucose after 30 min was almost plateaued indicating a significant impaired glucose tolerance (Fig. 1b, closed circles). Hypoxic exposure decreased the fasting glucose levels in both control (open triangles) and T2D (closed triangles) groups (Fig. 1b); however, T2D mice still developed impaired glucose tolerance under hypoxic condition. Hypoxia significantly decreased body weight in T2D, but not in control mice (Fig. 1c).

In comparison to CN mice, DN mice exhibited a slight, but statistically significant, increase in RVSP under normoxic conditions (Fig. 1d and 1e, left panel). Under hypoxic conditions, however, the hypoxia-induced increase in RVSP was significantly enhanced in DH mice compared to CH mice (Fig. 1d and 1e, right panel). These data provide strong evidence that the severity of chronic hypoxia-induced PH is significantly enhanced in diabetic mice; the enhanced HPH is associated with an impaired glucose tolerance in diabetic mice.

Effect of chronic hypoxia exposure on OGTT and RVSP in KK mice

To further confirm that HPH is enhanced in diabetic mice, we repeated the experiments shown in Fig. 2 using a genetically modified T2D mouse model, the KK mice. Fig. 2a shows the time course of the experiment. In the wild-type (WT) normoxia (WN) group, the mice were housed under normoxic conditions for 10 weeks before experimentation. In the genetically modified diabetic (KK) normoxia (KN) group, the mice were housed in the same room as WN mice under normoxic conditions for 10 weeks before the experiment. In the WT hypoxia (WH) group, mice were placed in a normobaric hypoxic chamber at the age of 6 weeks and exposed to hypoxia (10% O_2) for 4 weeks before experimentation. In the KK hypoxia (KH) group, the mice were placed in a normobaric hypoxic chamber at the age of 6 weeks and exposed to hypoxia (10% O_2) for 4 weeks before experimentation (Fig. 2a).

In WT normoxia (WN) mice, the plasma glucose declined rapidly 30 min after initial intake of glucose (Fig. 2b, open circles), whereas in genetically modified diabetic (KK) normoxia mice (KN), the glucose tolerance was impaired as shown by the significantly inhibited glucose decline in blood (Fig. 2b, closed circles). Hypoxic exposure significantly decreased the fasting glucose levels in both WH and KH mice. However, there was a significant difference of glucose tolerance between WH and KH mice after exposure to hypoxia (Fig. 2b). Hypoxic exposure significantly decreased body weight in both control and diabetic mice (Fig. 2c).

In comparison to WN mice, KN mice exhibited a significantly higher RVSP (approximately 30% increase) (Fig. 2d and 2e, left panel). The hypoxia-induced increase in RVSP was significantly enhanced in KH mice than in WH mice (Fig. 2d and 2e, right panel). Consistent with the data shown in the inducible T2D mice, these data further demonstrate that hypoxia-induced PH is significantly enhanced in diabetes. The enhanced HPH in diabetic mice may result from unique functional and structural changes in PAs due to diabetes.

Hypoxic exposure occludes small branches in control and T2D mice

Pulmonary vascular remodeling characterized by concentric pulmonary arterial wall thickening and intraluminal obliteration is a major cause for the increased PVR and PAP. A decrease in vascular density revealed by pulmonary angiography has been implicated in patients with idiopathic pulmonary arterial hypertension and in animals with experimental PH. To investigate whether the structural change in the pulmonary vasculature is involved in the enhanced HPH in diabetic mice, we compared the lung angiograms taken from the whole lungs of CN, DN, CH, and DH mice. Contrary to our expectation, the lung angiography data showed that pulmonary vascular density, determined by the numbers of vascular branch and junction and the total vascular length, was actually increased in DN mice in comparison to CN mice (Fig. 3a and 3b). Chronic exposure to hypoxia, however, significantly decreased the numbers of vascular branch and junction and the total vascular length in both control (CH) and diabetic (DH) mice (Fig. 3a and 3b). Although the numbers of vascular branch and junction and the total vascular length in CH and DH mice were the same under hypoxic conditions, the difference between DH mice and DN mice was significantly greater than the difference between CH mice and CN mice (Fig. 3c). These data suggest that chronic exposure to hypoxia can significantly reduce the pulmonary vascular density determined by lung angiography in both control and diabetic mice; however, the hypoxia-induced decrease in lung vascular density was significantly greater in diabetic mice than in control mice. Pulmonary vascular remodeling due to concentric vascular wall thickening and sustained pulmonary vasoconstriction due to inhibited EDR in PAs both contribute to decreased lung vascular density shown in lung angiograms. The next set of experiments was designed to determine whether inhibited EDR and mitochondrial ROS production are associated with the severe HPH in diabetic mice.

Scavenging mitochondrial O_2^- increases EDR in PAs of DH but not in PAs of CH

EDR in PAs and arterioles is an important mechanism involved in maintaining low PVR and PAP under normal

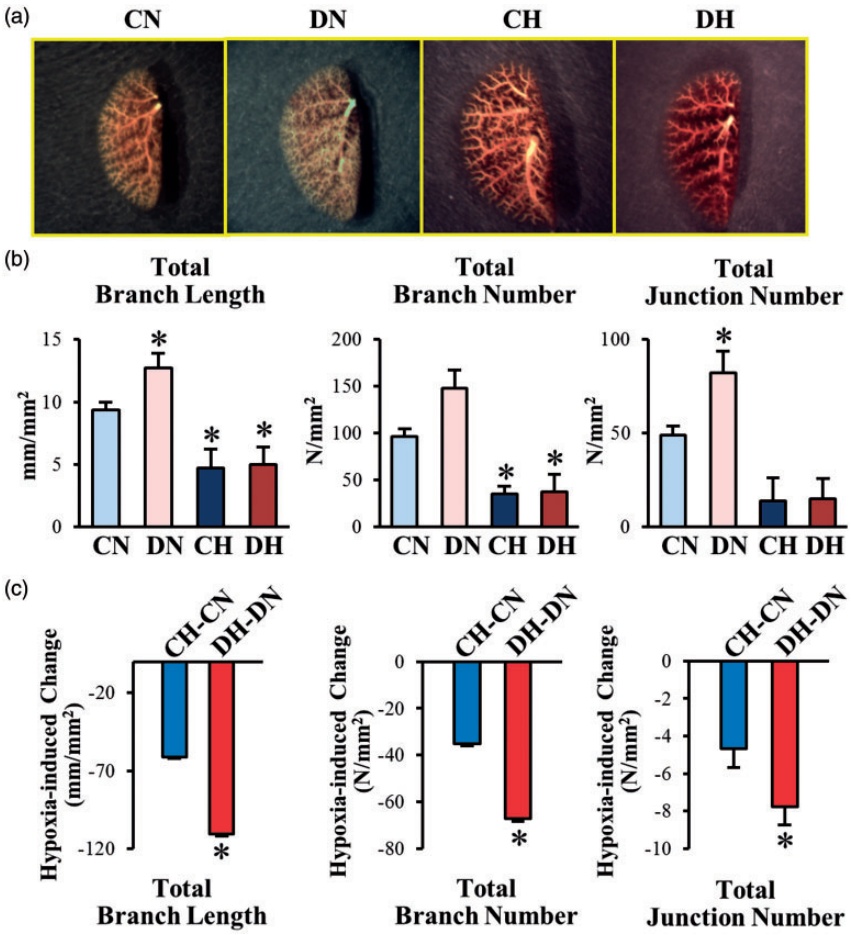

Fig. 3. T2D mice exhibit an increase in pulmonary arterial branches and chronic hypoxia-exposure decreases vascular branches in both control and T2D mice. (a) Representative angiography of the whole lung in control and T2D mice exposed to chronic normoxia or hypoxia. (b) Summarized data showing the total length of branches, the number of branches, and the number of junctions of vascular segments per square millimeter. CN, n = 6; DN, n = 7; CH, n = 4; DH; n = 5. Data are mean ± SEM. *$P < 0.05$ vs. CN.

and physiological conditions. EDR is mainly caused by the production and release of the endothelium-derived relaxing factor (EDRF), such as NO or prostacyclin (PGI_2), and via the induction of endothelium-dependent hyperpolarization. To examine whether inhibited EDR contributes to the enhanced HPH in diabetes, we compared the EDR in PA rings isolated from control and diabetic mice under hypoxic conditions. As shown in Fig. 4a, high K^+-mediated pulmonary vasoconstriction or increase in isometric tension in isolated PA rings, mainly due to membrane depolarization-induced opening of voltage-gated Ca^{2+} channels in PA smooth muscle cells, was comparable in CH mice and DH mice. These data suggest that the electromechanical coupling-induced contraction in isolated PA rings from control and diabetic mice was not affected by chronic hypoxia. However, the ACh-induced EDR was significantly attenuated in PA rings isolated from DH mice in comparison to the rings isolated from CH mice (Fig. 4b).

Mitochondrial ROS production has been implicated in the pulmonary arterial functions.[39–41] Pretreatment of mitoTempol (mitoT, 10 μM), a mitochondrial O_2^- scavenger, had a negligible effect on ACh-induced EDR in PA rings isolated from CH mice (Fig. 4c), but exhibited significantly enhanced EDR in PA rings isolated from DH mice (Fig. 4d). These data indicate that chelation of mitochondrial ROS is able to enhance ACh-induced EDR in PA rings from DH mice to the level similar to the EDR in PA rings isolated from CH mice. Given the results showing that mitoT (10 μM) had no effect on EDR in PA rings isolated from CH mice, these results imply that the excessive production of mitochondrial O_2^- attenuates PA relaxation in DH mice.

MPECs from DH exhibits increased mitochondrial ROS concentration and decreased SOD2 protein expression

Since mitoT treatment increased EDR in PA rings isolated from DH mice, we then expected that mitochondrial ROS generation might be increased in MPECs in DH mice. Indeed, as shown in Fig. 5, mitochondrial ROS concentration was significantly increased in MPEC isolated from DH mice in comparison to cells isolated from CH mice.

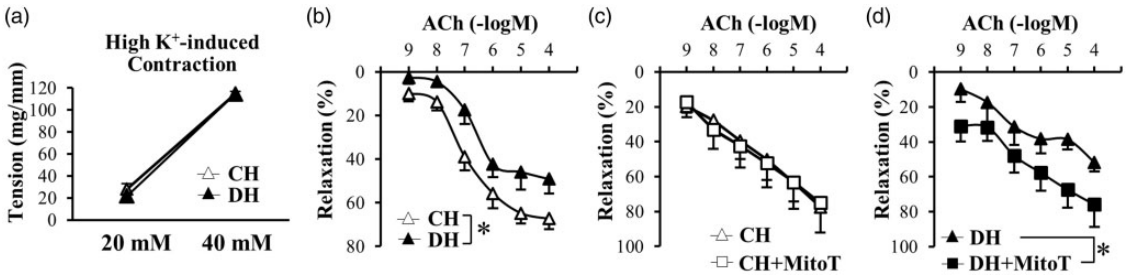

Fig. 4. (a, b) HighK^+-induced contraction is not different between PAs from CH and DH mice; however, EDR is significantly attenuated in DH-PAs compared to CH-PAs. (a) HighK^+-induced pulmonary arterial contraction. n = 5 per group. Data are mean ± SEM. (b) ACh-induced pulmonary arterial relaxation. CH, n = 7; DH, n = 6. Data are mean ± SEM. *$P < 0.05$ vs. CH. (c, d) Pretreatment of mitoT enhanced EDR in DH-PAs, but not in CH-PAs. (c) ACh-induced pulmonary arterial relaxation in the presence and absence of mitoT in CH. n = 4 per group. Data are mean ± SEM. (d) ACh-induced pulmonary arterial relaxation in the presence and absence of mitoT in DH. n = 4 per group. Data are mean ± SEM. *$P < 0.05$ vs. CH.

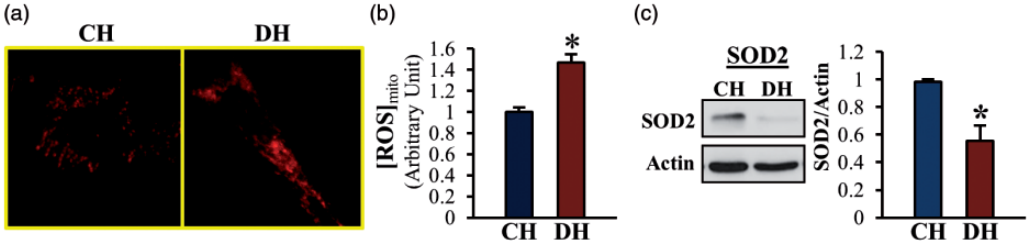

Fig. 5. $[ROS]_{mito}$ is significantly increased and SOD2 protein expression is significantly decreased in MPECs from DH mice compared to CH mice. (a) Cells were stained with MitoSOX (a mitochondrial ROS marker). (b) Summarized data showing $[ROS]_{mito}$ in CH and DH. CH, n = 155 cells; DH; n = 120 cells. Data are mean ± SEM. *$P < 0.05$ vs. CH. (c) Western blots showing SOD2 and actin protein levels (left panel). Actin was used as a loading control. Right columns show SOD2 protein level normalized to actin. n = 5 per group. Data are mean ± SEM. *$P < 0.05$ vs. CH.

The increased mitochondrial ROS concentration in MPECs from DH mice was associated with a significantly decreased protein level of SOD2, an important dismutase that decreases ROS level in the mitochondria (Fig. 5c). These data suggest that downregulated SOD2 protein expression level contributes to the increase in mitochondrial ROS concentration in MPEC of DH mice. The increased mitochondrial ROS in MPECs is, at least in part, responsible for the attenuated EDR in PA of DH mice. Sustained inhibition of endothelium-dependent pulmonary vasodilation then contributes to the development and progression of severe PH in diabetes under hypoxic conditions.

Discussion

Cardiovascular complications in diabetes are classified into two major groups: microvascular diseases and macrovascular diseases. Microvascular diseases in diabetes include retinopathy, nephropathy, and neuropathy; while macrovascular complications in diabetes include stroke and coronary heart disease. Therefore, the impacts of diabetes or high glucose on vascular function in the heart, brain, kidney, retina, and peripheral arteries have been extensively studied. It is, however, unclear whether diabetes affects the function of PAs, especially whether diabetic vascular endothelial dysfunction contributes to the development and progression of PH. There is strong clinical evidence showing that the development and/or progression of PH are more prominent in diabetic patient compared to control subjects,[1–5,42] but the specific cellular mechanisms potentially involved in the diabetes-associated severity of PH has not been explored. It has to be noted that the clinical reports investigating the relationship between PH and diabetes are all related to T2D, but not type 1 diabetes (T1D). Feeding a HF diet in ApoE knockout mice induces insulin resistance with mild, but significant, hyperglycemia. It was shown that ApoE-KO mice with a HF diet exhibited a significant increase in RVSP, right ventricular hypertrophy, and muscularization of PAs.[43] Kelley et al. also showed that 20 weeks of HF treatment in mice increased plasma insulin level that was associated with moderate increase of plasma glucose; these mice also exhibited significantly augmented RVSP, mean PAP, and pulmonary arterial muscularization.[44]

In this study, we used two different T2D mouse models, the inducible T2D mice and the genetically modified T2D

mice (KK mice), to test pulmonary functions. Our inducible T2D mice exhibited hyperglycemia, hyperinsulinemia, hyperlipidemia, abnormal glucose tolerance, and impaired insulin sensitivity.[34,36] This is a well-established mouse model to study T2D; the metabolic characteristics in this model are very close to those in human T2D induced by a Western diet.[35,36,45–47]

Under normoxic conditions, the inducible T2D mice and the KK mice both exhibited severe impairment of glucose tolerance. Chronic hypoxic exposure decreased fasting glucose levels in all mouse groups; however, the impaired glucose tolerance still remained in inducible T2D mice and KK mice (Figs. 1b and 2b). The body weight was significantly decreased in diabetic mice after hypoxic exposure (Figs. 1c and 2c). The effect of hypoxia on weight loss has been reported in humans and animals and it is more likely due to increased metabolism by hypoxia.[48–51]

In agreement with the other investigator's data, we also found that the inducible T2D mice and the KK mice exhibited slightly (but with statistical significance) increased RVSP in comparison to the control mice (Figs. 1d, 1e and 2d, 2e). The most important and novel finding in this study is that diabetes is a risk factor for developing severe PH in mice. We demonstrate that chronic exposure to hypoxia enhances the development and progression of PH in T2D mice. Moral-Sanz et al. also demonstrated that T1D rats exhibited the trend of enhanced hypoxia-induced PH (determined by hypoxia-induced increase in mean PAP) compared to the control rats. Their observations also suggest that macrophage infiltration is potentially an important mechanism by which hyperglycemia inhibits pulmonary vasodilation and ultimately leads to sustained pulmonary vasoconstriction and development of severe PH under hypoxic conditions.

PAP is a function of cardiac output (CO) and PVR. In patients and animals with hypoxia-induced PH, CO is not significantly augmented indicating that the increased PAP is mainly due to increased PVR. PVR is inversely proportional to the fourth power of intraluminal radius or diameter of PAs, so a very small decrease in intramural radius/diameter in PAs and arterioles would significantly increase PVR and PAP. The major causes that directly lead to increased PVR are thus sustained pulmonary vasoconstriction, concentric pulmonary vascular wall thickening, in situ thrombosis, and increased pulmonary vascular wall stiffness.

As shown in Fig. 3c, chronic hypoxia significantly decreased the pulmonary arterial branches which is expected from the data of increased RVSP under hypoxia in Fig. 1. However, there is no significant different between control mice exposed to hypoxia (CH) and T2D exposed to hypoxia (DH), suggesting that the significant difference of RVSP between CH and DH is not because of the change in pulmonary vascular branches.

Vascular tension is regulated by vasoconstriction and vasodilation; increased vascular constriction and decreased vascular relaxation lead to increased vascular tension. It has been demonstrated that EDR in patients with T2D and animals with experimental T2D is attenuated in various vascular systems;[10–12,14,15] however, it is still controversial whether pulmonary EDR is attenuated[52–55] or not changed[56,57] in animals with experimental HPH. The data from this study (Fig. 4a) demonstrated that high-K^+ induced contraction in PAs isolated from DH mice was not altered in comparison to PAs isolated from CH mice. However, EDR in isolated PAs was significantly impaired in DH mice compared to CH mice (Fig. 4b) or to CN and DN mice (supplemental data 1). Importantly, the attenuated pulmonary arterial EDR in DH mice could be rescued by pretreatment of the DH PAs with mitoT, a mitochondrial O_2^- scavenger. These results strongly suggest that excessive production of O_2^- in the mitochondria during hypoxia is an important mechanism involved in the inhibition of pulmonary arterial EDR in DH mice. By directly measuring ROS in mitochondria (Fig. 5a and 5b), we further confirmed that MPECs isolated from DH mice exhibited significantly higher level of $[ROS]_{mito}$ compared with MPECs isolated from CH mice.

Increased ROS production in mitochondria has been implicated in endothelial dysfunction in diabetes.[24,27,28,34] We also observed a significant increase in $[ROS]_{mito}$ in diabetic MPECs compared to control MPECs under normoxia (supplemental data 2). Whether $[ROS]_{mito}$ is increased or decreased during hypoxia or in hypoxia-induced PH is, however, still controversial. While some report that $[ROS]_{mito}$ is increased in PH,[32,58,59] some indicate that $[ROS]_{mito}$ is decreased in PH.[60–62] In the current study, we showed that chelation of mitochondrial ROS with mitoT (by pretreating the isolated pulmonary arterial rings with mitoT) did not affect EDR in PAs isolated from CH mice. These data suggest that mitochondrial ROS production is not excessive enough in the HPH model to attenuate EDR in PAs. The mouse lung or the lung vasculature seems to have sufficient capacity to efficiently eliminate ROS in the mitochondria under hypoxic conditions in control mice. In diabetic mice exposed to chronic hypoxia, however, mitochondrial ROS production seems to be excessive enough to inhibit pulmonary arterial EDR.

Mitochondrial $O_2^{-\bullet}$ is largely released to the matrix at complex I and to the intermembrane space at complex III in the electron transport chain. SOD catalyzes the dismutation of $O_2^{-\bullet}$ to hydrogen peroxide (H_2O_2). H_2O_2 is detoxified to H_2O in the matrix by catalase, the thioredoxin/thioredoxin peroxidase system, or the glutathione/glutathione peroxidase system. SOD2 is predominantly expressed in mitochondria, whereas SOD1 is expressed mainly in the cytoplasm. SOD2 protein expression is decreased in ECs[34] or arteries[63] in T2D mice. Our results from this study indicated that MPECs isolated from DH mice exhibited significantly lower expression level of SOD2 compared to CH mice. These data suggest that the downregulated SOD2 expression is one of the causes to increase mitochondrial ROS and, subsequently, attenuate EDR in PAs isolated from chronically hypoxic mice with T2D. The question is whether

scavenging mitochondrial $O_2^{-\bullet}$ is able to prevent the development of severe HPH in diabetes. Adesina et al. demonstrated that overexpression of mitochondria-tagged catalase, but not SOD2, decreased RVSP in chronically hypoxic mice, suggesting that decreasing mitochondrial $[O_2^{-\bullet}]$ and eliminating $O_2^{-\bullet}$ byproduct, H_2O_2, are both required to prevent the development of HPH.[32] Although our data show that mitoT sufficiently restores EDR in PAs isolated from DH mice toward the level similar to the PAs isolated from CH mice, it is possible that the treatment with SOD/catalase mimetic agents (e.g. EUK134, EUK207) would further improve EDR in DH mice and restore the inhibited EDR toward the level similar to the PAs isolated from CN mice.

In our angiography experiments (Fig. 3), it was unexpected to observe the significant increase of the numbers of pulmonary vascular branches and junctions in DN mice in comparison to CN mice (Fig. 3). An increased number of vascular branches should lead to a reduction of vascular resistance and a decrease in RVSP if other parameters are not altered (e.g. vascular reactivity). If PAs and/or arterioles are more prone to contraction because of inhibited EDR in diabetes, the effect of increased vascular branches and junctions on RVSP could be masked by decreased intraluminal radius. We found that there was a trend of decrease in EDR in DN mice compared to CN mice, although no statistical significance was achieved (supplemental data 1), suggesting that there might be another mechanism to explain the higher RVSP in DN compared to CN. We need to conduct further experiment to define the molecular mechanisms in which RVSP was significantly increased in DN compared to CN.

In conclusion, we demonstrate that diabetic mice are more susceptive to hypoxia and develop severe HPH due, at least in part, to the downregulation of SOD2, increase in $[ROS]_{mito}$ in MPECs, and inhibition of EDR in PAs in hypoxia-exposed diabetic mice compared to hypoxia-exposed control mice. These data also suggest that patients with diabetes are susceptible to pulmonary vascular disease associated with hypoxia.

Conflict of interest

The author(s) declare that there is no conflict of interest.

Funding

This work was supported by the grants of HL115578 (A. Makino) from the National Institutes of Health and BK2015041792 (M. Pan) from the Natural Science Foundation of Jiangsu Province and the Jiangsu Health International Exchange Program.

Supplemental Material

All supplemental material is available is available at http://journals.sagepub.com/doi/suppl/10.1086/690206

References

1. Movahed MR, Hashemzadeh M and Jamal MM. The prevalence of pulmonary embolism and pulmonary hypertension in patients with type II diabetes mellitus. *Chest* 2005; 128: 3568–3571.
2. Makarevich AE, Valevich VE and Pochtavtsev AU. Evaluation of pulmonary hypertension in COPD patients with diabetes. *Adv Med Sci* 2007; 52: 265–272.
3. Pugh ME, Robbins IM, Rice TW, et al. Unrecognized glucose intolerance is common in pulmonary arterial hypertension. *J Heart Lung Transplant* 2011; 30: 904–911.
4. Benson L, Brittain EL, Pugh ME, et al. Impact of diabetes on survival and right ventricular compensation in pulmonary arterial hypertension. *Pulm Circ* 2014; 4: 311–318.
5. Belly MJ, Tiede H, Morty RE, et al. HbA1c in pulmonary arterial hypertension: a marker of prognostic relevance? *J Heart Lung Transplant* 2012; 31: 1109–1114.
6. Tousoulis D, Kampoli AM and Stefanadis C. Diabetes mellitus and vascular endothelial dysfunction: current perspectives. *Curr Vasc Pharmacol* 2012; 10: 19–32.
7. Yang G, Lucas R, Caldwell R, et al. Novel mechanisms of endothelial dysfunction in diabetes. *J Cardiovasc Dis Res* 2010; 1: 59–63.
8. Roberts AC and Porter KE. Cellular and molecular mechanisms of endothelial dysfunction in diabetes. *Diab Vasc Dis Res* 2013; 10: 472–482.
9. Hadi HA, Carr CS and Al Suwaidi J. Endothelial dysfunction: cardiovascular risk factors, therapy, and outcome. *Vasc Health Risk Manag* 2005; 1: 183–198.
10. Chrissobolis S, Miller AA, Drummond GR, et al. Oxidative stress and endothelial dysfunction in cerebrovascular disease. *Front Biosci* 2011; 16: 1733–1745.
11. Li JM and Shah AM. Endothelial cell superoxide generation: regulation and relevance for cardiovascular pathophysiology. *Am J Physiol Regul Integr Comp Physiol* 2004; 287: R1014–1030.
12. Cho YE, Basu A, Dai AZ, et al. Coronary endothelial dysfunction and mitochondrial reactive oxygen species in type 2 diabetic mice. *Am J Physiol Cell Physiol* 2013; 305: C1033–C1040.
13. Estrada IA, Donthamsetty R, Debski P, et al. STIM1 restores coronary endothelial function in type 1 diabetic mice. *Circ Res* 2012; 111: 1166–1175.
14. Fitzgerald SM, Kemp-Harper BK, Tare M, et al. Role of endothelium-derived hyperpolarizing factor in endothelial dysfunction during diabetes. *Clin Exp Pharmacol Physiol* 2005; 32: 482–487.
15. Triggle CR, Ding H, Anderson TJ, et al. The endothelium in health and disease: a discussion of the contribution of non-nitric oxide endothelium-derived vasoactive mediators to vascular homeostasis in normal vessels and in type II diabetes. *Mol Cell Biochem* 2004; 263: 21–27.
16. Makino A, Platoshyn O, Suarez J, et al. Downregulation of connexin40 is associated with coronary endothelial cell dysfunction in streptozotocin-induced diabetic mice. *Am J Physiol Cell Physiol* 2008; 295: C221–230.
17. Klinger JR, Abman SH and Gladwin MT. Nitric oxide deficiency and endothelial dysfunction in pulmonary arterial hypertension. *Am J Respir Crit Care Med* 2013; 188: 639–646.
18. Giaid A and Saleh D. Reduced expression of endothelial nitric oxide synthase in the lungs of patients with pulmonary hypertension. *N Engl J Med* 1995; 333: 214–221.

19. Giaid A, Yanagisawa M, Langleben D, et al. Expression of endothelin-1 in the lungs of patients with pulmonary hypertension. *N Engl J Med* 1993; 328: 1732–1739.
20. Widlansky ME and Gutterman DD. Regulation of endothelial function by mitochondrial reactive oxygen species. *Antioxid Redox Signal* 2011; 15: 1517–1530.
21. Schmidt TS and Alp NJ. Mechanisms for the role of tetrahydrobiopterin in endothelial function and vascular disease. *Clin Sci (Lond)* 2007; 113: 47–63.
22. Damico R, Zulueta JJ and Hassoun PM. Pulmonary endothelial cell NOX. *Am J Respir Cell Mol Biol* 2012; 47: 129–139.
23. Li J, Chen X, Xiao W, et al. Mitochondria-targeted antioxidant peptide SS31 attenuates high glucose-induced injury on human retinal endothelial cells. *Biochem Biophys Res Commun* 2011; 404: 349–356.
24. Makino A, Scott BT and Dillmann WH. Mitochondrial fragmentation and superoxide anion production in coronary endothelial cells from a mouse model of type 1 diabetes. *Diabetologia* 2010; 53: 1783–1794.
25. Pangare M and Makino A. Mitochondrial function in vascular endothelial cell in diabetes. *J Smooth Muscle Res* 2012; 48: 1–26.
26. Joshi M, Kotha SR, Malireddy S, et al. Conundrum of pathogenesis of diabetic cardiomyopathy: role of vascular endothelial dysfunction, reactive oxygen species, and mitochondria. *Mol Cell Biochem* 2014; 386: 233–249.
27. Kizhakekuttu TJ, Wang J, Dharmashankar K, et al. Adverse alterations in mitochondrial function contribute to type 2 diabetes mellitus-related endothelial dysfunction in humans. *Arterioscler Thromb Vasc Biol* 2012; 32: 2531–2539.
28. Shenouda SM, Widlansky ME, Chen K, et al. Altered mitochondrial dynamics contributes to endothelial dysfunction in diabetes mellitus. *Circulation* 2011; 124: 444–453.
29. Afolayan AJ, Eis A, Teng RJ, et al. Decreases in manganese superoxide dismutase expression and activity contribute to oxidative stress in persistent pulmonary hypertension of the newborn. *Am J Physiol Lung Cell Mol Physiol* 2012; 303: L870–879.
30. Tang X, Luo YX, Chen HZ, et al. Mitochondria, endothelial cell function, and vascular diseases. *Front Physiol* 2014; 5: 175.
31. Sanders SP, Zweier JL, Kuppusamy P, et al. Hyperoxic sheep pulmonary microvascular endothelial cells generate free radicals via mitochondrial electron transport. *J Clin Invest* 1993; 91: 46–52.
32. Adesina SE, Kang BY, Bijli KM, et al. Targeting mitochondrial reactive oxygen species to modulate hypoxia-induced pulmonary hypertension. *Free Radic Biol Med* 2015; 87: 36–47.
33. Archer SL, Gomberg-Maitland M, Maitland ML, et al. Mitochondrial metabolism, redox signaling, and fusion: a mitochondria-ROS-HIF-1alpha-Kv1.5 O2-sensing pathway at the intersection of pulmonary hypertension and cancer. *Am J Physiol Heart Circ Physiol* 2008; 294: H570–578.
34. Cho YE, Basu A, Dai A, et al. Coronary endothelial dysfunction and mitochondrial reactive oxygen species in type 2 diabetic mice. *Am J Physiol Cell Physiol* 2013; 305: C1033–1040.
35. Fricovsky ES, Suarez J, Ihm SH, et al. Excess protein O-GlcNAcylation and the progression of diabetic cardiomyopathy. *Am J Physiol Regul Integr Comp Physiol* 2012; 303: R689–699.
36. Han Y, Cho YE, Ayon R, et al. SGLT inhibitors attenuate NO-dependent vascular relaxation in the pulmonary artery but not in the coronary artery. *Am J Physiol Lung Cell Mol Physiol* 2015; 309: L1027–1036.
37. Yamamura A, Guo Q, Yamamura H, et al. Enhanced Ca(2+)-sensing receptor function in idiopathic pulmonary arterial hypertension. *Circ Res* 2012; 111: 469–481.
38. Kalyanaraman B, Darley-Usmar V, Davies KJ, et al. Measuring reactive oxygen and nitrogen species with fluorescent probes: challenges and limitations. *Free Radic Biol Med* 2012; 52: 1–6.
39. Waypa GB, Marks JD, Mack MM, et al. Mitochondrial reactive oxygen species trigger calcium increases during hypoxia in pulmonary arterial myocytes. *Circ Res* 2002; 91: 719–726.
40. Yadav VR, Song T, Joseph L, et al. Important role of PLC-gamma1 in hypoxic increase in intracellular calcium in pulmonary arterial smooth muscle cells. *Am J Physiol Lung Cell Mol Physiol* 2013; 304: L143–151.
41. Wang YX and Zheng YM. ROS-dependent signaling mechanisms for hypoxic Ca(2+) responses in pulmonary artery myocytes. *Antioxid Redox Signal* 2010; 12: 611–623.
42. Abernethy AD, Stackhouse K, Hart S, et al. Impact of diabetes in patients with pulmonary hypertension. *Pulm Circ* 2015; 5: 117–123.
43. Hansmann G, Wagner RA, Schellong S, et al. Pulmonary arterial hypertension is linked to insulin resistance and reversed by peroxisome proliferator-activated receptor-gamma activation. *Circulation* 2007; 115: 1275–1284.
44. Kelley EE, Baust J, Bonacci G, et al. Fatty acid nitroalkenes ameliorate glucose intolerance and pulmonary hypertension in high-fat diet-induced obesity. *Cardiovasc Res* 2014; 101: 352–363.
45. Luo J, Quan J, Tsai J, et al. Nongenetic mouse models of non-insulin-dependent diabetes mellitus. *Metabolism* 1998; 47: 663–668.
46. Kusakabe T, Tanioka H, Ebihara K, et al. Beneficial effects of leptin on glycaemic and lipid control in a mouse model of type 2 diabetes with increased adiposity induced by streptozotocin and a high-fat diet. *Diabetologia* 2009; 52: 675–683.
47. Islam MS and Loots du T. Experimental rodent models of type 2 diabetes: a review. *Methods Find Exp Clin Pharmacol* 2009; 31: 249–261.
48. Palmer BF and Clegg DJ. Oxygen sensing and metabolic homeostasis. *Mol Cell Endocrinol* 2014; 397: 51–58.
49. Lippl FJ, Neubauer S, Schipfer S, et al. Hypobaric hypoxia causes body weight reduction in obese subjects. *Obesity (Silver Spring)* 2010; 18: 675–681.
50. Mekjavic IB, Amon M, Kolegard R, et al. The effect of normobaric hypoxic confinement on metabolism, gut hormones, and body composition. *Front Physiol* 2016; 7: 202.
51. Pulfrey SM and Jones PJ. Energy expenditure and requirement while climbing above 6,000 m. *J Appl Physiol (1985)* 1996; 81: 1306–1311.
52. Tulloh RM, Hislop AA, Boels PJ, et al. Chronic hypoxia inhibits postnatal maturation of porcine intrapulmonary artery relaxation. *Am J Physiol* 1997; 272: H2436–2445.
53. Li J, Shi QX, Fan R, et al. Vasculoprotective effect of U50,488H in rats exposed to chronic hypoxia: role of Akt-stimulated NO production. *J Appl Physiol (1985)* 2013; 114: 238–244.
54. Crawley DE, Zhao L, Giembycz MA, et al. Chronic hypoxia impairs soluble guanylyl cyclase-mediated pulmonary arterial relaxation in the rat. *Am J Physiol* 1992; 263: L325–332.

55. Coflesky JT and Evans JN. Pharmacologic properties of isolated proximal pulmonary arteries after seven-day exposure to in vivo hyperoxia. *Am Rev Respir Dis* 1988; 138: 945–951.
56. Moral-Sanz J, Lopez-Lopez JG, Menendez C, et al. Different patterns of pulmonary vascular disease induced by type 1 diabetes and moderate hypoxia in rats. *Exp Physiol* 2012; 97: 676–686.
57. Kroigaard C, Kudryavtseva O, Dalsgaard T, et al. K(Ca)3.1 channel downregulation and impaired endothelium-derived hyperpolarization-type relaxation in pulmonary arteries from chronically hypoxic rats. *Exp Physiol* 2013; 98: 957–969.
58. Cawthon D, Beers K and Bottje WG. Electron transport chain defect and inefficient respiration may underlie pulmonary hypertension syndrome (ascites)-associated mitochondrial dysfunction in broilers. *Poult Sci* 2001; 80: 474–484.
59. Alhawaj R, Patel D, Kelly MR, et al. Heme biosynthesis modulation via delta-aminolevulinic acid administration attenuates chronic hypoxia-induced pulmonary hypertension. *Am J Physiol Lung Cell Mol Physiol* 2015; 308: L719–728.
60. Dromparis P, Paulin R, Sutendra G, et al. Uncoupling protein 2 deficiency mimics the effects of hypoxia and endoplasmic reticulum stress on mitochondria and triggers pseudohypoxic pulmonary vascular remodeling and pulmonary hypertension. *Circ Res* 2013; 113: 126–136.
61. Sutendra G, Dromparis P, Wright P, et al. The role of Nogo and the mitochondria-endoplasmic reticulum unit in pulmonary hypertension. *Sci Transl Med* 2011; 3: 88ra55.
62. Bonnet S, Michelakis ED, Porter CJ, et al. An abnormal mitochondrial-hypoxia inducible factor-1alpha-Kv channel pathway disrupts oxygen sensing and triggers pulmonary arterial hypertension in fawn hooded rats: similarities to human pulmonary arterial hypertension. *Circulation* 2006; 113: 2630–2641.
63. Liu B, Kuang L and Liu J. Bariatric surgery relieves type 2 diabetes and modulates inflammatory factors and coronary endothelium eNOS/iNOS expression in db/db mice. *Can J Physiol Pharmacol* 2014; 92: 70–77.